



ELSEVIER

Available online at [www.sciencedirect.com](http://www.sciencedirect.com)



Applied Numerical Mathematics 49 (2004) 187–205



APPLIED  
NUMERICAL  
MATHEMATICS

[www.elsevier.com/locate/apnum](http://www.elsevier.com/locate/apnum)

## Approximating local averages of fluid velocities: The equilibrium Navier–Stokes equations

Adrian Dunca<sup>a,1</sup>, Volker John<sup>b,2</sup>, William Layton<sup>a,\*,1</sup>

<sup>a</sup> *Department of Mathematics, University of Pittsburgh, Pittsburgh, PA 15260, USA*

<sup>b</sup> *Institut für Analysis und Numerik, Otto-von-Guericke-Universität Magdeburg, Postfach 4120,  
39016 Magdeburg, Germany*

---

### Abstract

In the approximation of higher Reynolds number flow problems, the usual approach is to seek to approximate suitable velocity averages rather than the pointwise fluid velocity itself. We consider an approach to this question wherein the averages are local, spatial averages computed with the Gaussian filter (as in large eddy simulation) and the averages are approximated without using either turbulent closure models or wall laws. The approach we consider is a (underresolved) direct numerical simulation followed by postprocessing to extract accurate flow averages. *A priori* and *a posteriori* estimates are given for  $\|g_\delta * (\mathbf{u} - \mathbf{u}^h)\|_0$  which can give guidance for the coupling between the averaging radius  $\delta$  and the mesh width  $h$ . Numerical experiments support the error estimates and illustrate the adaptive grid refinement procedure. Our analysis and experiments are for the equilibrium case which is a step towards but still far from the actual case of a turbulent flow simulation.

© 2003 IMACS. Published by Elsevier B.V. All rights reserved.

*Keywords:* Large eddy simulation; Postprocessing; Convergence of the finite element method

---

---

\* Corresponding author.

*E-mail addresses:* [ardst21@pitt.edu](mailto:ardst21@pitt.edu) (A. Dunca), [john@mathematik.uni-magdeburg.de](mailto:john@mathematik.uni-magdeburg.de) (V. John), [wjl@pitt.edu](mailto:wjl@pitt.edu) (W. Layton).

*URLs:* <http://www-ian.math.uni-magdeburg.de/home/john/> (V. John), <http://www.math.pitt.edu/~wjl> (W. Layton).

<sup>1</sup> Partially supported by NSF grants DMS 9972622, INT 9814115 and DMS 0107627.

<sup>2</sup> Partially supported by the Deutsche Forschungsgemeinschaft (DFG) under the grant JO 329/4-1.

## 1. Introduction

The velocity and pressure  $(\mathbf{u}, p)$  in an equilibrium flow of a viscous, incompressible fluid satisfy the steady state Navier–Stokes equations

$$\begin{aligned} -\nu \Delta \mathbf{u} + (\mathbf{u} \cdot \nabla) \mathbf{u} + \nabla p &= \mathbf{f} && \text{in } \Omega, \\ \nabla \cdot \mathbf{u} &= 0 && \text{in } \Omega, \\ \mathbf{u} &= \mathbf{0} && \text{on } \partial \Omega, \\ \int_{\Omega} p \, d\mathbf{x} &= 0, \end{aligned} \tag{1}$$

where  $\nu$  is the kinematic viscosity,  $\Omega \subset \mathbb{R}^d$ ,  $d = 2, 3$ , is a bounded, regular domain,  $\mathbf{u} : \Omega \rightarrow \mathbb{R}^d$  is the velocity,  $p : \Omega \rightarrow \mathbb{R}$  is the pressure and  $\mathbf{f} : \Omega \rightarrow \mathbb{R}^d$  is the force driving the flow. The Reynolds number of the flow is  $\mathcal{O}(\nu^{-1})$ .

Many flow simulations (even for equilibrium problems) are by nature underresolved. In those cases it is normal to seek not to compute  $\mathbf{u}$  but rather local averages  $\bar{\mathbf{u}}$  of  $\mathbf{u}$ . An example is to define  $\bar{\mathbf{u}} = g_{\delta} * \mathbf{u}$ , where  $g_{\delta}$  is a user-selected filter with filter width  $\delta$  with  $0 < \text{mesh width} < \delta < 1$ , see [31] for an overview on filters applied in computations. One very common choice, which we make herein, is filtering with a Gaussian. The usual approach to approximate various flow averages is to average the Navier–Stokes equations (1), to model the arising Reynolds stress tensor  $\mathbb{R}(\mathbf{u}, \mathbf{u}) := \overline{\mathbf{u}\mathbf{u}^T} - \bar{\mathbf{u}}\bar{\mathbf{u}}^T$  in terms of  $\bar{\mathbf{u}}$ , i.e.,  $\mathbb{R}(\mathbf{u}, \mathbf{u}) \approx \mathbb{T}(\bar{\mathbf{u}}, \bar{\mathbf{u}})$ , to model the boundary behavior of the flow averages and then to solve approximately the resulting continuum model, which is, hopefully, an approximation to  $\bar{\mathbf{u}}$ .

This usual method leads to very difficult problems of finding a closure model with accuracy and universality and finding near wall models or wall laws for complex boundaries. At the present time, in spite of intense research efforts over many years, solutions to these two problems which are both accurate and universal continue to be elusive. Thus, there is a need to develop complementary approaches, such as the one begun in [22], which avoid the issues of closure and wall laws.

Even within the usual approach of large eddy simulation (LES) the following question arises. How is the accuracy of modeling steps to be assessed? The current gold standard is to take a (necessarily) lower Reynolds number simulation (a DNS) which is reliable, compute  $\mathbf{u}^h$ , then  $\bar{\mathbf{u}}^h$  and compare it to the model's approximate solution  $\mathbf{w}^h$ . An intermediate approach to evaluation is to take a DNS approximation  $\mathbf{u}^h$  and compute the modeling residual  $\|\mathbb{R}(\mathbf{u}, \mathbf{u}) - \mathbb{T}(\bar{\mathbf{u}}, \bar{\mathbf{u}})\|$ . In either approach, one difficulty is that fully reliable flow simulations are only possible for lower Reynolds numbers whereas the targeted physical problem occurs at higher Reynolds numbers. However, in either approach to validation, only reliable approximations to  $\bar{\mathbf{u}}$  and not to  $\mathbf{u}$  are required. Thus by using an adaptive procedure to produce assured accuracy in flow averages, it should be possible to provide reliable DNS data for higher Reynolds numbers for velocity averages than for velocities. Exactly this goal of developing adaptive methods for a computed flow's local spatial averages was attacked in [22] for the simplest flow problem, the Stokes problem.

In the present paper, we continue the development of these methods for higher (but not high) Reynolds numbers by studying non-linear equilibrium flow problems. The smoothing properties of convolution with a Gaussian have interesting consequences in the final estimates obtained in [22] and herein. Recently, very interesting results have been obtained by Hoffman [14,15] on the related question of estimating mesh cell averages of space–time, SUPG approximations of time dependent flow problems. It is easy to

forecast that there are many more interesting developments yet to come on the question of approximating reliably velocity averages at Reynolds numbers for which reliable pointwise velocity approximations are not possible.

The usual (physical) critique of the approach we study herein (underresolved DNS  $\rightarrow \mathbf{u}^h \rightarrow$  post-processing  $\rightarrow \overline{\mathbf{u}^h}$ ) is that an accumulation of energy in the smallest resolved scales in  $\mathbf{u}^h$  will occur. However, with the proper choice of  $\delta$ , averaging will remove oscillations caused by energy accumulation. On the other hand, it is also easy to include in an analysis a subgrid model incorporated into the discretization. The a posteriori estimates separate in terms which naturally decompose into modeling residual and numerical residual terms evaluated at the approximate solution, a typical effect observed also in [9,14,15] for example. This is illustrated in Section 5.

This paper contains both a priori error estimates and a posteriori estimates for velocity averages in Section 3 (using preliminaries collected in Section 2). Section 4 gives numerical tests of the predicted rates of convergence and the adaptive algorithm. For the former, we have selected test problems within the analytical hypotheses of the convergence theorem and for the latter one beyond them (the driven cavity problem).

The non-linear, equilibrium problem (considered herein) is far from the goal of simulating accurately the generation, interaction and decay of the large structures in a turbulent flow. At this point, it is perhaps useful to review briefly the challenges and the possible next steps to the time dependent problem of the post processing approach.

The estimates herein strongly exploit smoothing properties of the filter selected. Thus, at the start the fundamental issue arises of space versus space–time filtering as the most useful definition of the large scales in a turbulent flow. There is a lively discussion based on physics and fluid mechanics of exactly this question in the LES community and the answer is not yet clear. Because of the issue of time stepping, a choice of the exact realization of the post processing idea must also be made. There are three natural choices.

The first natural realization is the simple plan of a DNS over  $[0, T_{\text{final}}]$  which gives  $\mathbf{u}^h(t)$  and from which  $g * \mathbf{u}^h(t)$  can be computed on  $[0, T_{\text{final}}]$ . It is possible that, in the sense of flow statistics, a similar picture to the equilibrium case might hold: non-physical energy piled up near the cutoff frequency is removed by filtering, leaving (statistical) accuracy in the large scales with accuracy increasing as one moves further from the cutoff length scale. On the other hand, in the sense of pointwise behavior, the picture is likely much more complex. Many turbulent flows have localized regions of intense backscatter (roughly speaking, energy transfer from the possibly corrupted small scales to the large scales). This is one interpretation of the genesis of large scale numerical artifacts studied, e.g., in Brown and Minion [3] and Drikakis and Smolarkiewicz [6]. Another interpretation is that leading order truncation error terms contribute numerical vorticity which grows in these unstable regions [6]. Because of this effect, the prospect for pointwise accuracy of this first approach is highly unclear.

The second natural approach is to use post processing each time step: given  $\mathbf{u}^h(t_n)$ , filter this to obtain  $g * \mathbf{u}^h(t_n)$  and use this in the time stepping to obtain  $\mathbf{u}^h(t_{n+1})$ . This approach is closely related to, among other algorithms, the spectral vanishing viscosity method of Mayday and Tadmor [27] and the filtering stabilization of spectral element methods studied by Fisher and Mullen [29,10]. Precisely this second approach has recently been tested in [7]. It was, as expected, overly diffusive and non-linear modifications were necessary to obtain quality results. Thus, modifications of this second approach are clearly needed.

The above “non-linear modifications” in [7] suggest an implicit LES model. Thus, the third option is to explore an, as yet unknown, synthesis of adaptivity, post processing for high-frequency error reduction

and LES modeling for low frequency accuracy. There is a lot of interesting recent work on adaptivity and LES modeling, for, e.g., [9,14,15]. Finding the correct mix of these is the third approach and an exciting research problem.

## 2. Notations and mathematical preliminaries

Standard notations of Lebesgue and Sobolev spaces are used throughout this paper. The inner product in  $(L^2(\Omega))^d$ ,  $d = 1, 2, 3$  is denoted by  $(\cdot, \cdot)$ , the norm in  $(L^2(\Omega))^d$  by  $\|\cdot\|_0$ , the norm in  $(H^k(\Omega))^d$  by  $\|\cdot\|_k$ , the seminorm in  $(H^k(\Omega))^d$  by  $|\cdot|_k$  and the norms in Lebesgue spaces  $(L^p(\Omega))^d$ ,  $1 \leq p \leq \infty$ ,  $p \neq 2$  by  $\|\cdot\|_{L^p}$ . Bilinear forms and norms in subdomains  $\omega \subset \Omega$  are marked by an additional index, e.g.,  $(\cdot, \cdot)_\omega$  or  $\|\cdot\|_{0,\omega}$ . Norms of other spaces are marked by subscribing the name of the space at the norm symbol. As usual,

$$\begin{aligned} H_0^1(\Omega) &= \{v \in H^1(\Omega) : v|_{\partial\Omega} = 0\}, \\ L_0^2(\Omega) &= \{q \in L^2(\Omega) : (q, 1) = 0\}. \end{aligned}$$

Let  $V = (H_0^1(\Omega))^d$  and  $Q = L_0^2(\Omega)$ . We define the bilinear and trilinear form

$$a(\mathbf{u}, \mathbf{v}) = \nu(\nabla \mathbf{u}, \nabla \mathbf{v}), \quad b(\mathbf{u}, \mathbf{v}, \mathbf{w}) = ((\mathbf{u} \cdot \nabla) \mathbf{v}, \mathbf{w}).$$

The variational formulation of the Navier–Stokes equations (1) is to find a pair  $(\mathbf{u}, p) \in V \times Q$  such that

$$a(\mathbf{u}, \mathbf{v}) + b(\mathbf{u}, \mathbf{u}, \mathbf{v}) - (p, \nabla \cdot \mathbf{v}) + (\nabla \cdot \mathbf{u}, q) = (\mathbf{f}, \mathbf{v}), \quad (2)$$

for all  $(\mathbf{v}, q) \in V \times Q$ .

Let  $\mathcal{T}^h$  denote a decomposition of  $\Omega$  into mesh cells. We denote by  $h_K$  the diameter of a mesh cell  $K$ , by  $h_E$  the diameter of a face  $E$ , and we set  $h = \max_{K \in \mathcal{T}^h} \{h_K\}$ . Each family of triangulations is assumed to be admissible and shape regular in the usual sense, e.g., [4].

With the mesh  $\mathcal{T}^h$ , we can construct conforming velocity-pressure finite element spaces  $V^h \times Q^h$  with  $V^h \subset V$  and  $Q^h \subset Q$ . These spaces are assumed to satisfy the inf–sup or Babuška–Brezzi condition, i.e., there exists a constant  $\beta > 0$  independent of the triangulation such that

$$\inf_{q^h \in Q^h} \sup_{\mathbf{v}^h \in V^h} \frac{(q^h, \nabla \cdot \mathbf{v}^h)}{\|q^h\|_0 \|\nabla \mathbf{v}^h\|_0} \geq \beta > 0. \quad (3)$$

The discrete Navier–Stokes problem consists in finding a pair  $(\mathbf{u}^h, p^h) \in V^h \times Q^h$  such that

$$a(\mathbf{u}^h, \mathbf{v}^h) + b(\mathbf{u}^h, \mathbf{u}^h, \mathbf{v}^h) - (p^h, \nabla \cdot \mathbf{v}^h) + (\nabla \cdot \mathbf{u}^h, q^h) = (\mathbf{f}, \mathbf{v}^h), \quad (4)$$

for all  $(\mathbf{v}^h, q^h) \in V^h \times Q^h$ .

We assume the following regularity of the solution of (2) and approximation properties of the finite element spaces

$$\left. \begin{aligned} &\mathbf{u} \in (H^{k+1}(\Omega))^d \cap V, \quad p \in H^k(\Omega) \cap Q, \quad k \geq 1, \\ &V^h \text{ contains piecewise polynomials of degree } k, \\ &Q^h \text{ contains piecewise polynomials of degree } k - 1. \end{aligned} \right\} \quad (5)$$

For a wide variety of velocity-pressure finite element spaces satisfying (3), the following optimal a priori error estimates have been proven under the assumption (5), see, e.g., [12],

$$\left. \begin{aligned} \|\nabla(\mathbf{u} - \mathbf{u}^h)\|_0 + \|p - p^h\|_0 &\leq ch^k (|\mathbf{u}|_{k+1} + |p|_k), \\ \|\mathbf{u} - \mathbf{u}^h\|_0 &\leq ch^{k+1} (|\mathbf{u}|_{k+1} + |p|_k), \end{aligned} \right\} \quad (6)$$

where  $c$  denotes throughout this paper a generic constant independent of  $T^h$  and  $(\mathbf{u}^h, p^h)$ .

We will consider in this paper an average of the error which is defined by a convolution with the Gaussian filter function

$$g_\delta(\mathbf{x}) = \left(\frac{6}{\delta^2\pi}\right)^{d/2} \exp\left(-\frac{6}{\delta^2}|\mathbf{x}|^2\right), \quad (7)$$

where  $|\mathbf{x}|$  denotes the Euclidean norm of  $\mathbf{x} \in \mathbb{R}^d$  and  $\delta$  is the filter width. A function to be convolved with  $g_\delta$  is continued by zero outside  $\Omega$ .

**Lemma 2.1.** *Let  $f_1, f_2 \in L^2(\Omega)$ , then*

$$(g_\delta * f_1, f_2) = (f_1, g_\delta * f_2), \quad (8)$$

and

$$\|g_\delta * f_1\|_k \leq c(k)\delta^{-k} \|f_1\|_0. \quad (9)$$

**Proof.** First, we note that by a direct calculation (and a change of variables in the integral) it follows immediately that

$$\|\partial_\alpha g_\delta\|_{L^1(\mathbb{R}^d)} \leq c(|\alpha|)\delta^{-|\alpha|}, \quad (10)$$

for any multi-index  $\alpha$ .

Using the symmetry of  $g_\delta$ , Fubini's theorem and that  $f_1, f_2$  are extended trivially off  $\Omega$  give

$$\begin{aligned} (g_\delta * f_1, f_2) &= \int_{\mathbb{R}^d} \left( \int_{\mathbb{R}^d} g_\delta(\mathbf{y} - \mathbf{x}) f_1(\mathbf{x}) \, d\mathbf{x} \right) f_2(\mathbf{y}) \, d\mathbf{y} \\ &= \int_{\mathbb{R}^d} \left( \int_{\mathbb{R}^d} g_\delta(\mathbf{x} - \mathbf{y}) f_2(\mathbf{y}) \, d\mathbf{y} \right) f_1(\mathbf{x}) \, d\mathbf{x} \\ &= (f_1, g_\delta * f_2)_{L^2(\mathbb{R}^d)} = (f_1, g_\delta * f_2). \end{aligned}$$

We have  $g_\delta * f_1 \in C^\infty(\mathbb{R}^d)$  and  $\partial_\alpha(g_\delta * f_1) = (\partial_\alpha g_\delta) * f_1$  for any multi-index  $\alpha$ , see Rudin [30, Theorem 6.35]. It follows from  $f_1 \equiv 0$  outside  $\Omega$  and Young's inequality for convolutions

$$\|\partial_\alpha(g_\delta * f_1)\|_{L^2(\mathbb{R}^d)} \leq \|\partial_\alpha g_\delta\|_{L^1(\mathbb{R}^d)} \|f_1\|_0.$$

Inequality (9) follows now by applying (10).  $\square$

We wish to estimate  $\|g_\delta * (\mathbf{u} - \mathbf{u}^h)\|_0$ . To this end, we consider the linearized adjoint problem to the Navier–Stokes equations with right side  $g_\delta * \boldsymbol{\psi}$ , where  $\boldsymbol{\psi} \in (L^2(\Omega))^d$  is arbitrary but fixed. Let  $(\mathbf{u}, p)$

be the solution of (2). Then, the weak formulation of the adjoint problem linearized at  $(\mathbf{u}, p)$  is to find  $(\boldsymbol{\phi}, \lambda) \in V \times Q$  such that

$$a(\mathbf{v}, \boldsymbol{\phi}) + b(\mathbf{u}, \mathbf{v}, \boldsymbol{\phi}) + b(\mathbf{v}, \mathbf{u}, \boldsymbol{\phi}) - (q, \nabla \cdot \boldsymbol{\phi}) + (\nabla \cdot \mathbf{v}, \lambda) = (g_\delta * \boldsymbol{\psi}, \mathbf{v}), \quad (11)$$

for all  $(\mathbf{v}, q) \in V \times Q$ . Problem (11) is assumed to be  $H^{\hat{k}+1}$ -regular, i.e., the solution  $(\boldsymbol{\phi}, \lambda)$  exists and satisfies

$$\|\boldsymbol{\phi}\|_{\hat{k}+1} + \|\lambda\|_{\hat{k}} \leq c(\mathbf{u}, \nu) \|g_\delta * \boldsymbol{\psi}\|_{\hat{k}-1}. \quad (12)$$

From (9) follows

$$\|\boldsymbol{\phi}\|_{\hat{k}+1} + \|\lambda\|_{\hat{k}} \leq c(\mathbf{u}, \nu, \hat{k}) \delta^{-\hat{k}+1} \|\boldsymbol{\psi}\|_0. \quad (13)$$

Let  $I_{V^h} : V \rightarrow V^h$  and  $I_{Q^h} : Q \rightarrow Q^h$  be interpolation operators satisfying local interpolation error estimates for all mesh cells  $K \in \mathcal{T}^h$

$$\begin{aligned} \|\mathbf{v} - I_{V^h}(\mathbf{v})\|_{0,K} &\leq ch_K^k \|\mathbf{v}\|_{k, \tilde{\omega}(K)} & \forall \mathbf{v} \in V \cap (H^k(\Omega))^d, \\ \|\nabla(\mathbf{v} - I_{V^h}(\mathbf{v}))\|_{0,K} &\leq ch_K^{k-1} \|\mathbf{v}\|_{k, \tilde{\omega}(K)} & \forall \mathbf{v} \in V \cap (H^k(\Omega))^d, \\ \|\mathbf{v} - I_{V^h}(\mathbf{v})\|_{0,E} &\leq ch_E^{k-1/2} \|\mathbf{v}\|_{k, \tilde{\omega}(E)} & \forall \mathbf{v} \in V \cap (H^k(\Omega))^d, \forall E \subset \partial K, \\ \|q - I_{Q^h}(q)\|_{0,K} &\leq ch_K^k \|q\|_{k, \tilde{\omega}(K)} & \forall q \in Q \cap H^k(\Omega), \\ \|q - I_{Q^h}(q)\|_{0,E} &\leq ch_E^{k-1/2} \|q\|_{k, \tilde{\omega}(K)} & \forall q \in Q \cap H^k(\Omega), \forall E \subset \partial K. \end{aligned} \quad (14)$$

If  $k \geq 2$ , the Lagrange interpolation operator can be taken for  $I_{V^h}$  and  $I_{Q^h}$ . In this case, we have  $\omega(K) = K$  and  $\omega(E) = \{K : E \subset \partial K\}$ . For  $k < 2$ , one can use the Clément interpolation operator, [5]. In this case,  $\omega(K)$  is the set of mesh cells which contains  $K$  and all mesh cells whose closure has a point with the closure of  $K$  in common. The set  $\omega(E)$  is the union of all mesh cells whose closure has a common point with the closure of face  $E$ . By the shape regularity assumption on the triangulations, the maximal number of mesh cells in  $\omega(K)$  and  $\omega(E)$  is bounded independent of  $\mathcal{T}^h$ . Thus, from the local interpolation error estimates follow global ones

$$\begin{aligned} \|\mathbf{v} - I_{V^h}(\mathbf{v})\|_0 &\leq ch^k \|\mathbf{v}\|_k & \forall \mathbf{v} \in V \cap (H^k(\Omega))^d, \\ \|\nabla(\mathbf{v} - I_{V^h}(\mathbf{v}))\|_0 &\leq ch^{k-1} \|\mathbf{v}\|_k & \forall \mathbf{v} \in V \cap (H^k(\Omega))^d, \\ \|q - I_{Q^h}(q)\|_0 &\leq ch^k \|q\|_k & \forall q \in Q \cap H^k(\Omega). \end{aligned} \quad (15)$$

The existence of interpolation operators fulfilling the local error estimates (14) is known for mesh cells which originate from a reference mesh cell by an affine transformation, e.g., for  $d$ -simplices or parallelepipeds. The interpolation error of general quadrilateral and hexahedral finite elements with non-affine transformations was studied in [28].

The jump  $[\mathbf{v}^h]_E$  of a function  $\mathbf{v}^h$  across a face  $E$  is defined by

$$[\mathbf{v}^h]_E := \begin{cases} \lim_{t \rightarrow +0} \{\mathbf{v}^h(\mathbf{x} + t\mathbf{n}_E) - \mathbf{v}^h(\mathbf{x} - t\mathbf{n}_E)\} & E \not\subset \partial\Omega, \\ \lim_{t \rightarrow +0} \{-\mathbf{v}^h(\mathbf{x} - t\mathbf{n}_E)\} & E \subset \partial\Omega, \end{cases}$$

where  $\mathbf{n}_E$  is a normal unit vector on  $E$  and  $\mathbf{x} \in E$ . If  $E \subset \partial\Omega$ , we choose the outer normal, otherwise  $\mathbf{n}_E$  has an arbitrary but fixed orientation. With that, every face  $E$  which separates two neighbouring mesh

cells  $K_1$  and  $K_2$  is associated with a uniquely oriented normal (for definiteness from  $K_1$  to  $K_2$ ) and the jump of a function  $\mathbf{v}^h \in V^h$  across a face  $E$  is  $[\mathbf{v}^h]_E = \mathbf{v}^h|_{K_2} - \mathbf{v}^h|_{K_1}$ . If  $\mathbf{v} \in V$ , then we know from the trace theorem  $\mathbf{v}|_E \in (H^{1/2}(E))^d$  and for this reason  $[\mathbf{v}]_E = \mathbf{0}$  a.e.

### 3. Error estimates for the large eddies

In this section, we give both *á priori* (Proposition 3.1) and *a posteriori* (Proposition 3.5) error estimates for the most basic realization of our idea, using the usual, centered, Galerkin finite element method with no extra stabilization, eddy viscosity or upwinding. These estimates show that the large eddies contain extra accuracy whenever  $\delta \gg h$ . These estimates are valid for general and shape regular meshes (and thus do not depend upon superconvergence properties) but do depend upon the smoothing properties of the convolution by a Gaussian. Thus, they should be extensible to the Pao filter and the sharp spectral cut-off filter but not to the box filter.

**Proposition 3.1** (*Á priori error estimate*). *Let  $(\mathbf{u}, p)$  be the solution of the Navier–Stokes equations (2),  $(\mathbf{u}^h, p^h)$  be the solution of the discrete Navier–Stokes equations (4) and  $\delta$  be the filter width of the Gaussian filter (7). Suppose  $(\mathbf{u}, p)$  possesses the regularity given in (5), the finite element spaces fulfill the inf–sup condition (3) and the regularity (12) of the solution of the linearized adjoint problem (11) is  $1/2 < \hat{k} \leq k$ . Denote  $\mathbf{e} = \mathbf{u} - \mathbf{u}^h$ , then there are positive constants  $c(\mathbf{u}, \nu, \hat{k})$  and  $c(\mathbf{u}, \nu, \hat{k}, \varepsilon)$  such that for any  $\varepsilon > 0$*

$$\begin{aligned} \|g_\delta * \mathbf{e}\|_0 &\leq c(\mathbf{u}, \nu, \hat{k}) \left(\frac{h}{\delta}\right)^{\hat{k}} \delta (\|\nabla \mathbf{e}\|_0 + \|p - p^h\|_0 + \|\nabla \cdot \mathbf{e}\|_0 + h^{1/2} \|\nabla \mathbf{u}\|_0 \|\nabla \mathbf{e}\|_0 + h^{1/2} \|\nabla \mathbf{e}\|_0^2) \\ &\quad + c(\mathbf{u}, \nu, \hat{k}, \varepsilon) \delta^{1/2-\varepsilon} \|\mathbf{e}\|_0 \|\nabla \mathbf{e}\|_0. \end{aligned} \tag{16}$$

**Proof.** Choosing the test functions in (2) from the finite element spaces and subtracting (4) from (2) gives the Galerkin orthogonality

$$a(\mathbf{e}, \mathbf{v}^h) + b(\mathbf{u}, \mathbf{u}, \mathbf{v}^h) - b(\mathbf{u}^h, \mathbf{u}^h, \mathbf{v}^h) - (p - p^h, \nabla \cdot \mathbf{v}^h) + (\nabla \cdot \mathbf{e}, q^h) = 0,$$

for all  $(\mathbf{v}^h, q^h) \in V^h \times Q^h$ . A straightforward calculation gives

$$b(\mathbf{u}, \mathbf{u}, \mathbf{v}^h) - b(\mathbf{u}^h, \mathbf{u}^h, \mathbf{v}^h) = b(\mathbf{e}, \mathbf{u}, \mathbf{v}^h) + b(\mathbf{u}, \mathbf{e}, \mathbf{v}^h) - b(\mathbf{e}, \mathbf{e}, \mathbf{v}^h), \tag{17}$$

such that

$$a(\mathbf{e}, \mathbf{v}^h) + b(\mathbf{e}, \mathbf{u}, \mathbf{v}^h) + b(\mathbf{u}, \mathbf{e}, \mathbf{v}^h) - b(\mathbf{e}, \mathbf{e}, \mathbf{v}^h) - (p - p^h, \nabla \cdot \mathbf{v}^h) + (\nabla \cdot \mathbf{e}, q^h) = 0. \tag{18}$$

We set  $\mathbf{v} = \mathbf{e}$  and  $q = p - p^h$  in the linearized dual problem (11) and subtract (18). This gives for all  $(\mathbf{v}^h, q^h) \in V^h \times Q^h$

$$\begin{aligned} (g_\delta * \boldsymbol{\psi}, \mathbf{e}) &= a(\mathbf{e}, \boldsymbol{\phi} - \mathbf{v}^h) + b(\mathbf{u}, \mathbf{e}, \boldsymbol{\phi} - \mathbf{v}^h) + b(\mathbf{e}, \mathbf{u}, \boldsymbol{\phi} - \mathbf{v}^h) + b(\mathbf{e}, \mathbf{e}, \mathbf{v}^h) \\ &\quad - (p - p^h, \nabla \cdot (\boldsymbol{\phi} - \mathbf{v}^h)) + (\nabla \cdot \mathbf{e}, \lambda - q^h). \end{aligned} \tag{19}$$

We wish to bound the terms on the right side of (19). Therefore, we choose  $\mathbf{v}^h = I_{V^h}(\boldsymbol{\phi})$  and  $q^h = I_{Q^h}(\lambda)$ . By applying the Cauchy–Schwarz inequality, the interpolation error estimate (15) and estimate (13), we get

$$\begin{aligned}
|a(\mathbf{e}, \boldsymbol{\phi} - I_{V^h}(\boldsymbol{\phi}))| &\leq \nu \|\nabla \mathbf{e}\|_0 \|\nabla(\boldsymbol{\phi} - I_{V^h}(\boldsymbol{\phi}))\|_0 \\
&\leq c\nu h^{\hat{k}} \|\boldsymbol{\phi}\|_{\hat{k}+1} \|\nabla \mathbf{e}\|_0 \leq c(\mathbf{u}, \nu, \hat{k}) \left(\frac{h}{\delta}\right)^{\hat{k}} \delta \|\nabla \mathbf{e}\|_0 \|\boldsymbol{\psi}\|_0, \\
|(p - p^h, \nabla \cdot (\boldsymbol{\phi} - I_{V^h}(\boldsymbol{\phi})))| &\leq c(\mathbf{u}, \nu, \hat{k}) \left(\frac{h}{\delta}\right)^{\hat{k}} \delta \|p - p^h\|_0 \|\boldsymbol{\psi}\|_0, \\
|(\nabla \cdot \mathbf{e}, \lambda - I_{Q^h}(\lambda))| &\leq c(\mathbf{u}, \nu, \hat{k}) \left(\frac{h}{\delta}\right)^{\hat{k}} \delta \|\nabla \cdot \mathbf{e}\|_0 \|\boldsymbol{\psi}\|_0.
\end{aligned}$$

Using Hölder's inequality, the Sobolev imbeddings  $H^1(\Omega) \rightarrow L^6(\Omega)$  and  $H^{1/2}(\Omega) \rightarrow L^3(\Omega)$ , the interpolation of  $H^{1/2}(\Omega)$  between  $L^2(\Omega)$  and  $H^1(\Omega)$  (see [1, Theorem 4.17]), the interpolation error estimate (15) and the estimate (13) yield

$$\begin{aligned}
|b(\mathbf{u}, \mathbf{e}, \boldsymbol{\phi} - I_{V^h}(\boldsymbol{\phi}))| &\leq \|\mathbf{u}\|_{L^6} \|\nabla \mathbf{e}\|_0 \|\boldsymbol{\phi} - I_{V^h}(\boldsymbol{\phi})\|_{L^3} \leq c \|\nabla \mathbf{u}\|_0 \|\nabla \mathbf{e}\|_0 \|\boldsymbol{\phi} - I_{V^h}(\boldsymbol{\phi})\|_{1/2} \\
&\leq c \|\nabla \mathbf{u}\|_0 \|\nabla \mathbf{e}\|_0 \|\boldsymbol{\phi} - I_{V^h}(\boldsymbol{\phi})\|_0^{1/2} \|\nabla(\boldsymbol{\phi} - I_{V^h}(\boldsymbol{\phi}))\|_0^{1/2} \\
&\leq c \|\nabla \mathbf{u}\|_0 \|\nabla \mathbf{e}\|_0 h^{\hat{k}+1/2} \|\boldsymbol{\phi}\|_{\hat{k}+1} \leq c(\mathbf{u}, \nu, \hat{k}) \left(\frac{h}{\delta}\right)^{\hat{k}} h^{1/2} \delta \|\nabla \mathbf{u}\|_0 \|\nabla \mathbf{e}\|_0 \|\boldsymbol{\psi}\|_0.
\end{aligned}$$

One obtains in the same way

$$|b(\mathbf{e}, \mathbf{u}, \boldsymbol{\phi} - I_{V^h}(\boldsymbol{\phi}))| \leq c(\mathbf{u}, \nu, \hat{k}) \left(\frac{h}{\delta}\right)^{\hat{k}} h^{1/2} \delta \|\nabla \mathbf{u}\|_0 \|\nabla \mathbf{e}\|_0 \|\boldsymbol{\psi}\|_0.$$

The last trilinear term in (19) is split into two parts

$$b(\mathbf{e}, \mathbf{e}, I_{V^h}(\boldsymbol{\phi})) = b(\mathbf{e}, \mathbf{e}, I_{V^h}(\boldsymbol{\phi}) - \boldsymbol{\phi}) + b(\mathbf{e}, \mathbf{e}, \boldsymbol{\phi}).$$

For the first of these terms, we get in the analogous way as above

$$|b(\mathbf{e}, \mathbf{e}, I_{V^h}(\boldsymbol{\phi}) - \boldsymbol{\phi})| \leq c(\mathbf{u}, \nu, \hat{k}) \left(\frac{h}{\delta}\right)^{\hat{k}} h^{1/2} \delta \|\nabla \mathbf{e}\|_0^2 \|\boldsymbol{\psi}\|_0.$$

The second term is estimated by using the Sobolev imbedding  $H^{3/2+\varepsilon}(\Omega) \rightarrow L^\infty(\Omega)$ ,  $\varepsilon > 0$  and (13)

$$\begin{aligned}
|b(\mathbf{e}, \mathbf{e}, \boldsymbol{\phi})| &\leq \|\mathbf{e}\|_0 \|\nabla \mathbf{e}\|_0 \|\boldsymbol{\phi}\|_{L^\infty} \leq c(\varepsilon) \|\mathbf{e}\|_0 \|\nabla \mathbf{e}\|_0 \|\boldsymbol{\phi}\|_{3/2+\varepsilon} \\
&\leq c(\mathbf{u}, \nu, \hat{k}, \varepsilon) \delta^{1/2-\varepsilon} \|\mathbf{e}\|_0 \|\nabla \mathbf{e}\|_0 \|\boldsymbol{\psi}\|_0.
\end{aligned} \tag{20}$$

The Riesz representation theorem and (8) yield

$$\|g_\delta * \mathbf{e}\|_0 = \sup_{\boldsymbol{\psi} \in (L^2(\Omega))^d} \frac{(g_\delta * \mathbf{e}, \boldsymbol{\psi})}{\|\boldsymbol{\psi}\|_0} = \sup_{\boldsymbol{\psi} \in (L^2(\Omega))^d} \frac{(g_\delta * \boldsymbol{\psi}, \mathbf{e})}{\|\boldsymbol{\psi}\|_0}. \tag{21}$$

Thus, collecting estimates and dividing by  $\|\boldsymbol{\psi}\|_0$  gives the error estimate (16).  $\square$

**Remark 3.2.** Let the approximation assumptions (5) be fulfilled. Then, the last factor of the first term in (16) behaves like  $\mathcal{O}(h^{\hat{k}})$ .

Let  $\delta = ch^\alpha$  with  $\alpha \in [0, 1]$ . The order of convergence given by (16) is  $\mathcal{O}(h^{k+1+(1-\alpha)(\hat{k}-1)})$ . If  $\hat{k} > 1$  and  $\alpha < 1$ , the convergence of the large eddies defined by convolution with  $g_\delta$  is faster than the convergence of the velocity as given in (6).

If  $\alpha = 1$ , then the order of convergence for the large eddies is the same as for the velocity. This is consistent since the filter width corresponds to the mesh size in this case. Flow structures smaller than the mesh size cannot be computed such that the mesh size gives a lower bound for the filter width. Thus, taking the filter width of the order of the mesh size must recover the results known for the velocity.

The last term in (16) is of order  $\mathcal{O}(h^{2k+1+\alpha(1/2-\varepsilon)})$  where  $\varepsilon > 0$ . This is a higher order term for any  $\alpha \in [0, 1]$ .

**Remark 3.3.** Estimate (16), which is true for  $d \in \{2, 3\}$ , can be improved for  $d = 2$  since the Sobolev imbeddings  $H^{2/3}(\Omega) \rightarrow L^6(\Omega)$ ,  $H^{1/3}(\Omega) \rightarrow L^3(\Omega)$  and  $H^{1+\varepsilon}(\Omega) \rightarrow L^\infty(\Omega)$ ,  $\varepsilon > 0$  hold. One obtains

$$\begin{aligned} \|g_\delta * \mathbf{e}\|_0 &\leq c(\mathbf{u}, \nu, \hat{k}) \left(\frac{h}{\delta}\right)^{\hat{k}} \delta (\|\nabla \mathbf{e}\|_0 + \|p - p^h\|_0 + \|\nabla \cdot \mathbf{e}\|_0 + h^{2/3} \|\nabla \mathbf{u}\|_0 \|\nabla \mathbf{e}\| + h^{2/3} \|\nabla \mathbf{e}\|_0^2) \\ &\quad + c(\mathbf{u}, \nu, \hat{k}, \varepsilon) \delta^{1-\varepsilon} \|\mathbf{e}\|_0 \|\nabla \mathbf{e}\|_0. \end{aligned}$$

However, the improvements occur only in higher order terms and the asymptotic order of convergence is the same as for  $d = 3$ , see Remark 3.2.

**Remark 3.4.** An alternative definition of the linearized dual problem: Find  $(\phi, \lambda) \in V \times Q$  such that

$$a(\mathbf{v}, \phi) + b(\mathbf{u}, \mathbf{v}, \phi) + b(\mathbf{v}, \mathbf{u}^h, \phi) - (q, \nabla \cdot \phi) + (\nabla \cdot \mathbf{v}, \lambda) = (g_\delta * \boldsymbol{\psi}, \mathbf{v}),$$

for all  $(\mathbf{v}, q) \in V \times Q$  would lead to the vanishing of the term  $b(\mathbf{e}, \mathbf{e}, \mathbf{v}^h)$  in (19) and to the last term in the error estimate (16). However, the constants in the stability estimate (12) and in the error estimate (16) would depend on  $\mathbf{u}^h$ , too. In addition, assuming a higher regularity of the solution of the linearized dual problem like in (12) requires in general sufficiently regular data. Regularity for  $\mathbf{u}$  can be assumed but the regularity for  $\mathbf{u}^h$  is restricted by the regularity of functions in the finite element space. In general, only  $\mathbf{u}^h \in (H^1(\Omega))^d$  is given.

**Proposition 3.5** (A posteriori error estimate). *Let the assumptions of Proposition 3.1 be fulfilled. Then, there are constants  $c(\mathbf{u}, \nu, \hat{k}) > 0$  and  $c(\mathbf{u}, \nu, \hat{k}, \varepsilon) > 0$  such that for any  $\varepsilon > 0$*

$$\|g_\delta * \mathbf{e}\|_0 \leq c(\mathbf{u}, \nu, \hat{k}) \left(\sum_{K \in \mathcal{T}^h} \eta_K^2\right)^{1/2} + c(\mathbf{u}, \nu, \hat{k}, \varepsilon) \delta^{1/2-\varepsilon} \|\mathbf{e}\|_0 \|\nabla \mathbf{e}\|_0, \tag{22}$$

with

$$\begin{aligned} \eta_K^2 &= \left(\frac{h_K}{\delta}\right)^{2\hat{k}} \delta^2 \left[ h_K^2 \|\mathbf{f} - (-\nu \Delta \mathbf{u}^h + (\mathbf{u}^h \cdot \nabla) \mathbf{u}^h + \nabla p^h)\|_{0,K}^2 \right. \\ &\quad \left. + \|\nabla \cdot \mathbf{u}^h\|_{0,K}^2 + \sum_{E \subset \partial K} \frac{h_E}{2} \|[-\nu \nabla \mathbf{u}^h \mathbf{n} + p^h \mathbf{n}]_E\|_{0,E}^2 \right]. \end{aligned} \tag{23}$$

**Proof.** Let  $\boldsymbol{\psi} \in (L^2(\Omega))^d$  be given and let  $(\phi, \lambda) \in (V, Q)$  be the solution of the linearized dual problem (11). The error equation (19), the identity (17) and (8) give

$$\begin{aligned}
 (\boldsymbol{\psi}, g_\delta * \mathbf{e}) &= a(\mathbf{e}, \boldsymbol{\phi} - \mathbf{v}^h) + b(\mathbf{u}, \mathbf{u}, \boldsymbol{\phi} - \mathbf{v}^h) - b(\mathbf{u}^h, \mathbf{u}^h, \boldsymbol{\phi} - \mathbf{v}^h) \\
 &\quad + (\lambda - q^h, \nabla \cdot \mathbf{e}) - (p - p^h, \nabla \cdot (\boldsymbol{\phi} - \mathbf{v}^h)) + b(\mathbf{e}, \mathbf{e}, \boldsymbol{\phi}).
 \end{aligned}
 \tag{24}$$

Let

$$\mathbf{r}_K = [\mathbf{f} - (-\nu \Delta \mathbf{u}^h + (\mathbf{u}^h \cdot \nabla) \mathbf{u}^h + \nabla p^h)]|_K$$

be the strong residual of the momentum equation restricted to the mesh cell  $K$ . Integration by parts of (24) mesh cell by mesh cell and  $\nabla \cdot \mathbf{u} = 0$  give

$$\begin{aligned}
 (\boldsymbol{\psi}, g_\delta * \mathbf{e}) &= \sum_{K \in \mathcal{T}^h} \left[ (\mathbf{r}_K, \boldsymbol{\phi} - \mathbf{v}^h)_K - (\lambda - q^h, \nabla \cdot \mathbf{u}^h)_K + \int_{\partial K} (-\nu \nabla \mathbf{u}^h \mathbf{n}_E + p^h \mathbf{n}_E) \cdot (\boldsymbol{\phi} - \mathbf{v}^h) \, ds \right] \\
 &\quad + b(\mathbf{e}, \mathbf{e}, \boldsymbol{\phi}).
 \end{aligned}$$

Choosing  $\mathbf{v}^h = I_{V^h}(\boldsymbol{\phi})$ ,  $q^h = I_{Q^h}(\lambda)$  and applying the local interpolation estimates (14) give

$$\begin{aligned}
 |(\boldsymbol{\psi}, g_\delta * \mathbf{e})| &\leq \sum_{K \in \mathcal{T}^h} \left[ h_K^{\hat{k}+1} \|\mathbf{r}_K\|_{0,K} \|\boldsymbol{\phi}\|_{\hat{k}+1, \omega(K)} + h_K^{\hat{k}} \|\nabla \cdot \mathbf{u}^h\|_{0,K} \|\lambda\|_{\hat{k}, \omega(K)} \right. \\
 &\quad \left. + \sum_{E \subset \partial K} \frac{h_E^{\hat{k}+1/2}}{2} \|[-\nu \nabla \mathbf{u}^h \mathbf{n} + p^h \mathbf{n}]_E\|_{0,E} \|\boldsymbol{\phi}\|_{\hat{k}+1, \omega(E)} \right] + |b(\mathbf{e}, \mathbf{e}, \boldsymbol{\phi})|.
 \end{aligned}$$

The shape regularity of  $\{\mathcal{T}^h\}$  guarantees that the number of mesh cells in  $\omega(K)$  and  $\omega(E)$  can be bounded independently of  $h$ . Thus, there is a constant independent of  $h$  such that

$$\begin{aligned}
 |(\boldsymbol{\psi}, g_\delta * \mathbf{e})| &\leq c \left( \sum_{K \in \mathcal{T}^h} \left[ h_K^{2\hat{k}+2} \|\mathbf{r}_K\|_{0,K}^2 + h_K^{2\hat{k}} \|\nabla \cdot \mathbf{u}^h\|_{0,K}^2 \right. \right. \\
 &\quad \left. \left. + \sum_{E \subset \partial K} \frac{h_E^{2\hat{k}+1}}{2} \|[-\nu \nabla \mathbf{u}^h \mathbf{n} + p^h \mathbf{n}]_E\|_{0,E}^2 \right] \right)^{1/2} (\|\boldsymbol{\phi}\|_{\hat{k}+1} + \|\lambda\|_{\hat{k}}) + |b(\mathbf{e}, \mathbf{e}, \boldsymbol{\phi})|.
 \end{aligned}$$

The application of the estimates (13) and (20), division by  $\|\boldsymbol{\psi}\|_0$ , the definition of the  $(L^2(\Omega))^d$  norm in (21) and  $h_E \leq h_K$  give (22).  $\square$

#### 4. Numerical studies

The approximate solutions we shall present are computed using the following algorithm. The Navier–Stokes equations (1) are linearized by a fixed point iteration. Let  $(\mathbf{u}^n, p^n)$  be the current iterate, then the next iterate is computed by solving

$$\begin{aligned}
 -\nu \Delta \mathbf{u}^{n+1} + (\mathbf{u}^n \cdot \nabla) \mathbf{u}^{n+1} + \nabla p^{n+1} &= \mathbf{0} && \text{in } \Omega, \\
 \nabla \cdot \mathbf{u}^{n+1} &= 0 && \text{in } \Omega, \\
 \mathbf{u}^{n+1} &= \mathbf{0} && \text{on } \partial\Omega, \\
 \int_{\Omega} p \, dx &= 0.
 \end{aligned}
 \tag{25}$$

The linear saddle point problem (25) is discretized by a finite element method. We will use so-called mapped finite elements, i.e., all finite elements are defined first on a reference cell  $\widehat{K}$  and the finite elements on an arbitrary mesh cell  $K$  are defined with the help of the reference map to the reference cell, see [23] for advantages of using this approach in finite element computations.

The cube  $(-1, 1)^d$  is used as reference cell  $\widehat{K}$  for quadrilateral and hexahedral mesh cells. The reference transformation from the closure of  $\widehat{K}$  onto the closure of a mesh cell  $K$  is denoted by  $F_K$ . For  $d = 3$ , we denote by  $Q_k(\widehat{K})$  and  $P_k(\widehat{K})$  the following sets of polynomials on  $\widehat{K}$

$$Q_k(\widehat{K}) := \left\{ \hat{q} = \sum_{i,j,l=0}^k a_{ijl} \hat{x}^i \hat{y}^j \hat{z}^l \right\}, \quad P_k(\widehat{K}) := \left\{ \hat{p} = \sum_{i,j,l=0}^{i+j+l \leq k} b_{ijl} \hat{x}^i \hat{y}^j \hat{z}^l \right\}.$$

The modifications for  $d = 2$  are obviously. The spaces on an arbitrary mesh cell  $K$  are given by

$$Q_k(K) := \{q = \hat{q} \circ F_K^{-1} : \hat{q} \in Q_k(\widehat{K})\},$$

$$P_k(K) := \{p = \hat{p} \circ F_K^{-1} : \hat{p} \in P_k(\widehat{K})\}$$

and the global finite element spaces by

$$Q_k := \{v \in H^1(\Omega) : v|_K \in Q_k(K)\}, \quad k \geq 1,$$

$$P_k^{\text{disc}} := \{v \in L^2(\Omega) : v|_K \in P_k(K)\}, \quad k \geq 1.$$

In our numerical tests, we use the inf–sup stable pairs of finite element spaces  $Q_k/Q_{k-1}$ ,  $k \geq 2$ , and  $Q_k/P_{k-1}^{\text{disc}}$ ,  $k \geq 2$ , on quadrilateral and hexahedral grids. As commonly done, the fact that the velocity space is a vector-valued function is not indicated in these notations.

For defining simplicial finite elements, the reference triangle with the vertices  $(0, 0)$ ,  $(1, 0)$ ,  $(0, 1)$  and the reference tetrahedron with the vertices  $(0, 0, 0)$ ,  $(1, 0, 0)$ ,  $(0, 1, 0)$ ,  $(0, 0, 1)$  are used. Using the spaces on the mesh cells given above, we define

$$P_k := \{v \in H^1(\Omega) : v|_K \in P_k(K)\}, \quad k \geq 1.$$

We use pairs of inf–sup stable finite element spaces  $P_k/P_{k-1}$ ,  $k \geq 2$ , on simplicial meshes.

In order to support the a priori error estimate (16), we have to compute the convolution of the error. Let  $\varphi \in L^2(\mathbb{R}^d)$ , then we obtain by applying the Fourier transform

$$\mathcal{F}(g_\delta * \varphi)(\mathbf{y}) = (\mathcal{F}(g_\delta)\mathcal{F}(\varphi))(\mathbf{y}) = \exp\left(-\frac{\delta^2}{24}|\mathbf{y}|^2\right)\mathcal{F}(\varphi)(\mathbf{y}).$$

Approximating the exponential by the subdiagonal Padé approximation

$$e^{ax} = \frac{1}{1+ax} + \mathcal{O}(a^2x^2),$$

neglecting terms of  $\mathcal{O}(\delta^4)$  and the inverse Fourier transform yield

$$\mathcal{F}(g_\delta * \varphi)(\mathbf{y}) = (\mathcal{F}(g_\delta)\mathcal{F}(\varphi))(\mathbf{y}) \approx \frac{1}{1 + \frac{|\mathbf{y}|^2}{24}\delta^2}\mathcal{F}(\varphi)(\mathbf{y}) = \mathcal{F}\left(\left(I - \frac{\delta^2}{24}\Delta\right)^{-1}\varphi\right)(\mathbf{y}),$$

from what follows

$$g_\delta * \varphi \approx \left(I - \frac{\delta^2}{24}\Delta\right)^{-1}\varphi. \tag{26}$$

We use the second order elliptic partial differential equation on the right side of (26) for approximating the convolution numerically. This is much more efficient than numerical quadrature, see [21]. If  $\varphi$  is given on a bounded domain, the second order elliptic partial differential equation is equipped with homogeneous Neumann boundary conditions as proposed in [11].

**Example 4.1** (2d example supporting the error estimates (16) and (22)). We consider the Navier–Stokes equations (1) in  $\Omega = (0, 1)^2$  with the prescribed solution  $\mathbf{u} = (u_1, u_2)$  and  $p$  given by

$$\begin{aligned} u_1 &= 2\pi \sin^3(\pi x) \sin(\pi y) \cos(\pi y), \\ u_2 &= -3\pi \sin^2(\pi x) \cos(\pi x) \sin^2(\pi y), \\ p &= \cos(\pi x) + \cos(\pi y) \end{aligned}$$

and  $Re = 10$ . This problem fits exactly into the framework of the analysis presented in Section 3. The order of convergence depends on the regularity  $\hat{k}$  of the dual problem given in (12). In the case of a polygonal domain, one can expect in general only  $\hat{k} = 1$ . However, the regularity might be higher for particular examples. The order of convergence obtained in the numerical studies suggest that  $\hat{k} = 3$  in this example. It follows from Remark 3.2 that for  $\delta = ch^\alpha$  the order of convergence expected for  $\|g_\delta * (\mathbf{u} - \mathbf{u}^h)\|_0$  is  $k + 2 - \alpha$  if  $k = 2$  and  $k + 3 - 2\alpha$  if  $k \geq 3$ .

The mesh width  $h$  for a given triangulation  $\mathcal{T}$  is defined by

$$h = \max_{K \in \mathcal{T}} h_K, \quad \text{where } h_K := \max_{\mathbf{x}, \mathbf{y} \in K} |\mathbf{x} - \mathbf{y}|$$

and the global error estimate by  $\eta = (\sum_K \eta_K^2)^{1/2}$  with  $\eta_K$  given by (23). Note that the a posteriori error estimate  $\eta$  is only useful if its order of convergence is the same as for the a priori error estimate (16).

Tables 1–4 present results for finite element discretizations with velocity spaces of order  $k$  and pressure spaces of order  $k - 1$ ,  $k \in \{2, 3, 4\}$  and different values of  $\delta$ . The computations were carried out on quadrilateral and triangular grids. The initial quadrilateral grid (level 0) consists of four squares of edge length 0.5. The initial triangular grid is obtained by dividing these squares from bottom left to top right.

All numerical tests coincide very well with the analytical results. The error estimator shows in all numerical tests the correct asymptotic order of convergence. However, the error is always overestimated in this example. The overestimation ranges from a factor of about 26 (Table 1) to nearly 400 (Table 4).

Table 1  
Example 4.1,  $Q_2/Q_1$  finite element discretization,  $\delta = 0.5$  ( $\alpha = 0$ )

Level	$\ \mathbf{u} - \mathbf{u}^h\ _0$		$\ g_\delta * (\mathbf{u} - \mathbf{u}^h)\ _0$		$\eta$	
0	5.840541e-1		1.631631e-1		1.173043e+01	
1	8.551689e-2	2.772	2.412399e-2	2.758	7.174224e-1	4.031
2	1.086894e-2	2.976	1.297768e-3	4.216	4.197971e-2	4.095
3	1.380864e-3	2.977	8.637593e-5	3.909	2.518792e-3	4.059
4	1.732925e-4	2.994	5.677399e-6	3.927	1.554372e-4	4.018
5	2.168210e-5	2.999	3.643621e-7	3.962	9.682313e-6	4.005
6	2.710897e-6	3.000	2.307744e-8	3.981	6.046293e-7	4.001
7	3.388818e-7	3.000	1.451969e-9	3.990	3.778124e-8	4.000
Theory		3.000		4.000		4.000

Table 2  
Example 4.1,  $P_3/P_2$  finite element discretization,  $\delta = h^{0.75}$

Level	$\ \mathbf{u} - \mathbf{u}^h\ _0$		$\ g_\delta * (\mathbf{u} - \mathbf{u}^h)\ _0$		$\eta$	
0	2.030502e-1		3.446956e-2		6.750303e+0	
1	1.940913e-2	3.387	4.348816e-3	2.987	2.677952e-1	4.656
2	1.216234e-3	3.996	1.387224e-4	4.970	1.189230e-2	4.493
3	7.764174e-5	3.969	4.951325e-6	4.808	5.249900e-4	4.502
4	4.902454e-6	3.985	1.958768e-7	4.660	2.322077e-5	4.499
5	3.070333e-7	3.997	8.207853e-9	4.577	1.026300e-6	4.500
6	1.918967e-8	4.000	3.498957e-10	4.552	4.535184e-8	4.500
Theory		4.000		4.500		4.500

Table 3  
Example 4.1,  $P_3/P_2$  finite element discretization,  $\delta = h$  ( $\alpha = 1$ )

Level	$\ g_\delta * (\mathbf{u} - \mathbf{u}^h)\ _0$		$\eta$	
0	3.789549e-2		8.027508e+0	
1	5.331715e-3	2.829	4.503760e-1	4.156
2	1.890456e-4	4.818	2.828482e-2	3.993
3	9.572364e-6	4.304	1.765849e-3	4.002
4	5.721758e-7	4.064	1.104572e-4	3.999
5	3.520322e-8	4.023	6.904097e-6	4.000
6	2.181624e-9	4.012	4.314618e-7	4.000
Theory		4.000		4.000

Table 4  
Example 4.1,  $Q_4/P_3^{\text{disc}}$  finite element discretization,  $\delta = h^{0.8}$

Level	$\ \mathbf{u} - \mathbf{u}^h\ _0$		$\ g_\delta * (\mathbf{u} - \mathbf{u}^h)\ _0$		$\eta$	
0	3.537659e-2		5.995522e-3		1.489979e+0	
1	1.231637e-3	4.844	1.236179e-4	5.600	3.945655e-2	5.239
2	3.971647e-5	4.955	2.499258e-6	5.628	9.527598e-4	5.372
3	1.254649e-6	4.984	5.678712e-8	5.460	2.250758e-5	5.404
4	3.932204e-8	4.996	1.345722e-9	5.399	5.325324e-7	5.401
5	1.229726e-9	4.999	3.202971e-11	5.393	1.260853e-8	5.400
Theory		5.000		5.400		5.400

**Example 4.2** (3d example supporting the error estimate (16)). Let  $\Omega = (0, 1)^3$  and let  $\mathbf{u} = (u_1, u_2, u_3)$  and  $p$  given by

$$u_1(x, y, z) = \sin(\pi x) \sin(\pi y) \sin(\pi z) + x^4 \cos(\pi y),$$

$$u_2(x, y, z) = \cos(\pi x) \cos(\pi y) \cos(\pi z) - 3y^3 z,$$

$$u_3(x, y, z) = \cos(\pi x) \sin(\pi y) \cos(\pi z) + \cos(\pi x) \sin(\pi y) \sin(\pi z) - 4x^3 z \cos(\pi y) + 4.5y^2 z^2,$$

$$p(x, y, z) = 3x - \sin(y + 4z) + c.$$

Table 5

Example 4.2,  $Q_2/P_1^{\text{disc}}$  finite element discretization, order of convergence for different choices of  $\delta$

Level	$\ \mathbf{u} - \mathbf{u}^h\ _0$		$\ g_\delta * (\mathbf{u} - \mathbf{u}^h)\ _0$ $\delta = h^{0.5}$		$\ g_\delta * (\mathbf{u} - \mathbf{u}^h)\ _0$ $\delta = 0.5$	
0	3.742528e-2		7.012790e-3		1.008274e-2	
1	4.478076e-3	3.063	7.600275e-4	3.206	8.531608e-4	3.563
2	5.343528e-4	3.067	6.406178e-5	3.569	6.249804e-5	3.771
3	6.569613e-5	3.024	4.774094e-6	3.746	4.232580e-6	3.884
4	8.173159e-6	3.007	3.300154e-7	3.855	2.748632e-7	3.945
5	1.020367e-6	3.002	2.184200e-8	3.917	1.750525e-8	3.973
Theory		3.000		3.500		4.000

The constant  $c$  is chosen such that  $p \in L_0^2(\Omega)$  and the right side  $\mathbf{f}$  is chosen such that  $(\mathbf{u}, p)$  fulfil the momentum equation in (1) for  $Re = 10$ . In contrast to (1), we have here a solution with non-homogeneous Dirichlet boundary conditions. As in Example 4.1, the numerical results suggest that the regularity of the dual problem (12) is given with  $\hat{k} \geq 2$ . Thus, the expected asymptotic order of convergence for  $\|g_\delta * (\mathbf{u} - \mathbf{u}^h)\|_0$  is  $k + 2 - \alpha$  if  $k = 2$  and  $\delta = ch^\alpha$ , see Remark 3.2.

The computations were carried out with the  $Q_2/P_1^{\text{disc}}$  finite element discretization on a hexahedral grid. The initial grid (level 0) consists of 8 cubes of edge length 0.5. On level 5, there are nearly 7.5 million degrees of freedom.

Table 5 presents the computed results. For fixed  $\delta$ , i.e.,  $\alpha = 0$ , the numerical results coincide well with the analytical prediction. For  $\delta = h^{0.5}$ , the order of convergence in the numerical tests is larger than the expected asymptotic value. We think that the grids are not yet sufficiently fine to be in the asymptotic regime in this case.

**Example 4.3** (2d examples investigating the adaptive refinement using the a posteriori error estimator).

The last numerical example shows that the large eddies can be computed on an adaptively refined grid with less degrees of freedom than the solution of the Galerkin discretization of the Navier–Stokes equations  $(\mathbf{u}^h, p^h)$  for the same stopping criterion on the global a posteriori error estimate.

We consider the driven cavity problem in 2d with  $Re = 1000$  in  $\Omega = (0, 1)^2$  and with  $\mathbf{f} = \mathbf{0}$ ,  $\mathbf{u} = (1, 0)^T$  for  $y = 1$  and no slip conditions on the other parts of the boundary, see Fig. 1 for an illustration of the flow. Since the restriction of  $\mathbf{u}$  to the boundary does not lie in  $H^{1/2}(\partial\Omega)$ , it follows that  $\mathbf{u} \notin H^1(\Omega)$ . Although the solution of the driven cavity problem is not sufficiently smooth to match the assumptions of Proposition 3.5, the behaviour of the a posteriori error estimator can be illustrated well with this example.

We used in the computations the  $P_2/P_1$  finite element discretization on a triangular grid. The coarsest level (level 0) consists of 32 equal triangles. This grid is refined twice uniformly (512 triangles) before the adaptive grid refinement based on the a posteriori error estimates (23) starts. In addition, we present results for the standard estimator for  $\|\mathbf{u} - \mathbf{u}^h\|_0$  where the local error estimate is given by

$$\eta_K^2 = h_K^4 \|\mathbf{f} - (-Re^{-1} \Delta \mathbf{u}^h + (\mathbf{u}^h \cdot \nabla) \mathbf{u}^h + \nabla p^h)\|_{0,K}^2 + h_K^2 \|\nabla \cdot \mathbf{u}^h\|_{0,K}^2 + \sum_{E \subset \partial K} \frac{h_E^3}{2} \|[-Re^{-1} \nabla \mathbf{u}^h \mathbf{n} + p^h \mathbf{n}]_E\|_{0,E}^2.$$

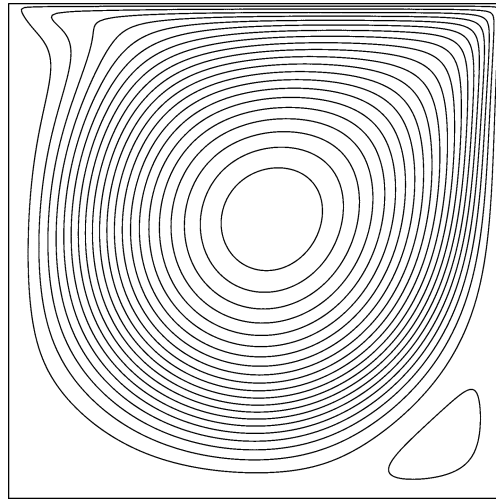


Fig. 1. Streamlines of the solution of the driven cavity problem.

Table 6  
Degrees of freedom of the meshes presented in Fig. 2

$\delta$	Degrees of freedom		
	Velocity	Pressure	All
standard $L^2$ -estimator	791624	99450	891074
0.1	186 108	23 470	209 578
0.3	141 014	17 784	158 798
0.6	105 730	13 354	119 084

The framework of deriving this error estimator is given, e.g., in [8]. The estimator for the large eddies, Proposition 3.5, has a similar form like this standard  $L^2$ -error estimator. Thus, it is easy to implement in an existing code which allows adaptive grid refinement with residual based a posteriori error estimators.

The algorithm used for choosing the mesh cells which should be refined is described in detail in [19]. After the computation of the error estimates on a triangulation  $\mathcal{T}$ , the following criteria for refining the mesh cells were applied. Given initially  $tol = 0.5$ .

- (1) A mesh cell  $K$  is refined if

$$\eta_K \geq tol \max_{K \in \mathcal{T}} \eta_K.$$

- (2) If in the first step less than 10% of the current mesh cells are marked for refinement,  $tol$  is decreased as long as at least 10% of the mesh cells will be refined.

We did not apply coarsening of mesh cells. The stopping criterion for the computations was  $\eta \leq 10^{-7}$ .

The results of the computations are presented in Table 6 and Fig. 2. The choice of different values of  $\delta$  leads to different final meshes. The larger the eddies to be approximated, the less degrees of freedom are necessary to fulfil the stopping criterion. Especially away from the singularities in the upper corners, the meshes obtained for the large eddies are coarser than the mesh obtained with the standard  $L^2$ -

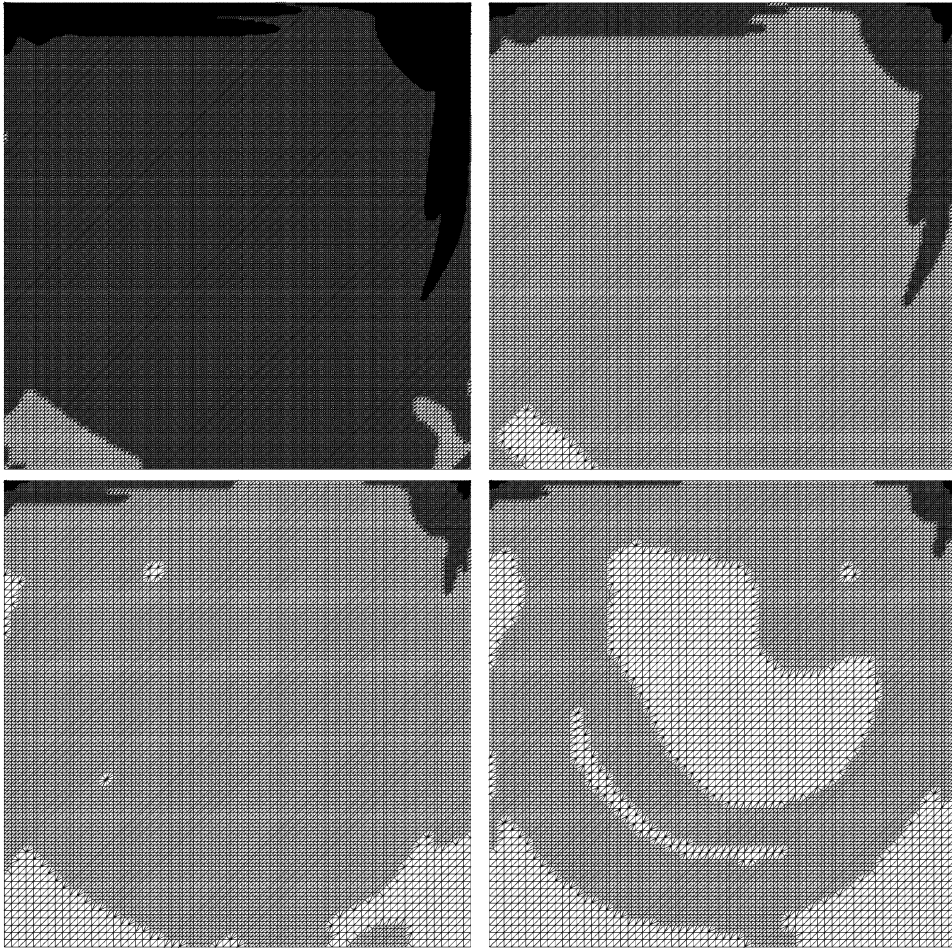


Fig. 2. Final grids for driven cavity example,  $\eta \leq 1e-7$ , standard  $L^2$ -error estimator, estimator  $\eta$  with  $\delta = 0.1$ ,  $\delta = 0.3$ ,  $\delta = 0.6$  (top left to bottom right).

error estimator. The sequence of meshes computed with the error estimators for the large eddies and the standard  $L^2$ -error estimator is also different. In comparison to the standard  $L^2$ -error estimator, the local estimates of the error estimators for the large eddies possess an additional weighting factor  $h_K$ . Thus, large mesh cells are refined earlier using the estimator for the large eddies.

## 5. Extensions to some stabilized discretizations

Naturally, at higher Reynolds numbers the usual (centered) Galerkin finite element method is improvable and there have been many interesting proposals for improvement. In this section, we aim to show that the framework of Section 3 can often be easily extended to account for the extra effects which arise in more complex discretizations. Since the theory of SUPG methods has been highly advanced, see [14,15], we focus herein on complementary methods which use subgrid stabilization of a general

form  $\nabla \cdot A^h(\mathbf{u}^h)$ . Thus, the discrete problem considered in this section is to find  $(\mathbf{u}^h, p^h) \in V^h \times Q^h$  satisfying

$$a(\mathbf{u}^h, \mathbf{v}^h) + (A^h(\mathbf{u}^h), \nabla \mathbf{v}^h) + b(\mathbf{u}^h, \mathbf{u}^h, \mathbf{v}^h) - (p^h, \nabla \cdot \mathbf{v}^h) + (\nabla \cdot \mathbf{u}^h, q^h) = (\mathbf{f}, \mathbf{v}^h), \tag{27}$$

for all  $(\mathbf{v}^h, q^h) \in V^h \times Q^h$ . Interesting examples of such  $A^h(\mathbf{u}^h)$  include the von Neumann–Richtmeyer/Smagorinsky/Ladyzhenskaya model, e.g., [32,25], the models developed in [18] and eddy viscosity models acting only on the smallest resolved scales, see Hughes et al. [17,16], Guermond [13] and [26,24].

**Proposition 5.1.** *Let  $(\mathbf{u}^h, p^h)$  satisfy (27) and let the assumptions of Proposition 3.5 hold. Then with  $\mathbf{e} = \mathbf{u} - \mathbf{u}^h$  and  $\eta_K$  given in (23), there are constants  $c(\mathbf{u}, \nu, \hat{k}) > 0$ ,  $c(\mathbf{u}, \nu, \hat{k}, \varepsilon) > 0$ ,  $h_0(\mathbf{u})$  such that for  $h \leq h_0(\mathbf{u})$  and for any  $\varepsilon > 0$*

$$\|g_\delta * \mathbf{e}\|_0 \leq c(\mathbf{u}, \nu, \hat{k}, \varepsilon) \left\{ \left( \sum_{K \in \mathcal{T}^h} \eta_K^2 \right)^{1/2} + \left( \sum_{K \in \mathcal{T}^h} \left( \frac{h_K}{\delta} \right)^{2\hat{k}} \delta^2 \|A^h(\mathbf{u}^h)\|_{0,K}^2 \right)^{1/2} + [\delta^{1/2-\varepsilon} \|\mathbf{e}\|_0 \|\nabla \mathbf{e}\|_0 + \delta^{-\hat{k}+1} \|A^h(\mathbf{u}^h)\|_{-\hat{k}}] \right\}. \tag{28}$$

**Proof.** A key ingredient to develop residual based a posteriori error estimates is Galerkin orthogonality [2,20]. The discretization (27) satisfies the approximate Galerkin orthogonality condition:

$$\begin{aligned} a(\mathbf{e}, \mathbf{v}^h) + b(\mathbf{e}, \mathbf{u}, \mathbf{v}^h) + b(\mathbf{u}, \mathbf{e}, \mathbf{v}^h) - b(\mathbf{e}, \mathbf{e}, \mathbf{v}^h) - (p - p^h, \nabla \cdot \mathbf{v}^h) + (\nabla \cdot \mathbf{e}, q^h) \\ = -(A^h(\mathbf{u}^h), \nabla \mathbf{v}^h) \quad \forall \mathbf{v}^h \in V^h. \end{aligned}$$

This is (18) modified by the term on the right side. Following the proof of Proposition 3.5, let  $\boldsymbol{\psi} \in L^2(\Omega)^d$  be given and let  $(\boldsymbol{\phi}, \lambda)$  be the solution of (11), the same estimates then give

$$\begin{aligned} |(\boldsymbol{\psi}, g_\delta * \mathbf{e})| \leq \left[ c(\mathbf{u}, \nu, \hat{k}) \left( \sum_{K \in \mathcal{T}^h} \eta_K^2 \right)^{1/2} + c(\mathbf{u}, \nu, \hat{k}, \varepsilon) \delta^{1/2-\varepsilon} \|\mathbf{e}\|_0 \|\nabla \mathbf{e}\|_0 \right] \|\boldsymbol{\psi}\|_0 \\ + |(A^h(\mathbf{u}^h), \nabla I_{V^h}(\boldsymbol{\phi}))|. \end{aligned}$$

Applying the triangle inequality to the last term on the right side gives

$$|(A^h(\mathbf{u}^h), \nabla I_{V^h}(\boldsymbol{\phi}))| \leq |(A^h(\mathbf{u}^h), \nabla \boldsymbol{\phi})| + |(A^h(\mathbf{u}^h), \nabla (I_{V^h}(\boldsymbol{\phi}) - \boldsymbol{\phi}))|.$$

The second term is bounded using (14) and (13)

$$|(A^h(\mathbf{u}^h), \nabla (I_{V^h}(\boldsymbol{\phi}) - \boldsymbol{\phi}))| \leq c(\mathbf{u}, \nu, \hat{k}) \left( \sum_{K \in \mathcal{T}^h} \left( \frac{h_K}{\delta} \right)^{2\hat{k}} \delta^2 \|A^h(\mathbf{u}^h)\|_{0,K}^2 \right)^{1/2} \|\boldsymbol{\psi}\|_0,$$

while the first term is bounded by

$$|(A^h(\mathbf{u}^h), \nabla \boldsymbol{\phi})| \leq c(\mathbf{u}, \nu, \hat{k}) \delta^{-\hat{k}+1} \|A^h(\mathbf{u}^h)\|_{-\hat{k}} \|\boldsymbol{\psi}\|_0.$$

The proof is completed by collecting estimates.  $\square$

**Remark 5.2.** The a posteriori error estimate can naturally be interpreted as being split into a “numerical residual” component (the first term in the right side of (28)), a “modeling residual” component (the second term) and a component which is asymptotically of higher order (the third bracketed component). This decoupling occurs in other a posteriori error estimates for approximations of models of stationary turbulence in [9]. The third, bracketed term in (28) is of higher order provided the basic method (27) is asymptotically convergent as  $h \rightarrow 0$ . Thus, a complete treatment requires an a priori convergence study of (27) which will necessarily depend upon the specific chosen form of  $A^h(\mathbf{u}^h)$ .

## References

- [1] R.A. Adams, Sobolev Spaces, Academic Press, New York, 1975.
- [2] L. Angermann, A posteriori error estimates for FEM with violated Galerkin orthogonality, Numer. Methods Partial Differential Equations 18 (2002) 241–259.
- [3] D.L. Brown, M.L. Minion, Performance of under-resolved two-dimensional incompressible flow simulations, J. Comput. Phys. 122 (1995) 165–183.
- [4] P.G. Ciarlet, Basic error estimates for elliptic problems, in: P.G. Ciarlet, J.L. Lions (Eds.), Handbook of Numerical Analysis II, North-Holland, Amsterdam, 1991, pp. 19–351.
- [5] Ph. Clément, Approximation by finite element functions using local regularization, RAIRO Anal. Numer. 2 (1975) 77–84.
- [6] D. Drikakis, P.K. Smolarkiewicz, On spurious vortical structures, J. Comput. Phys. 172 (2001) 309–325.
- [7] A. Dunca, Optimal design of fluid flow using subproblems reduced by large eddy simulation, Report, DEP, Argonne National Lab., Argonne, IL, 2002.
- [8] K. Eriksson, D. Estep, P. Hansbo, C. Johnson, Introduction to adaptive methods for differential equations, Acta Numer. (1995) 105–158.
- [9] V.J. Ervin, W.J. Layton, J.M. Maubach, Adaptive defect-correction methods for viscous incompressible flow problem, SIAM J. Numer. Anal. 37 (2000) 1165–1185.
- [10] P. Fischer, J. Mullen, Filter-based stabilization of spectral element methods, C. R. Acad. Sci. Paris Sér. I Math. 332 (2001) 265–270.
- [11] G.P. Galdi, W.J. Layton, Approximation of the larger eddies in fluid motion II: A model for space filtered flow, Math. Models Meth. Appl. Sci. 10 (3) (2000) 343–350.
- [12] V. Girault, P.-A. Raviart, Finite Element Methods for Navier–Stokes Equations, Springer, Berlin, 1986.
- [13] J.-L. Guermond, Stabilization of Galerkin approximations of transport equations by subgrid modeling, Modél. Math. Anal. Numér. 33 (1999) 1293–1316.
- [14] J. Hoffman, Adaptive finite element methods for turbulent flows, Preprint 08, Chalmers Finite Element Center, 2002.
- [15] J. Hoffman, Computational Modeling of Complex Flows, Ph.D. Thesis, Chalmers University of Technology, Göteborg, 2002.
- [16] T.J.R. Hughes, L. Mazzei, A.A. Oberai, A.A. Wray, The multiscale formulation of large eddy simulation: decay of homogeneous isotropic turbulence, Phys. Fluids 13 (2001) 505–512.
- [17] T.J.R. Hughes, A.A. Oberai, L. Mazzei, Large eddy simulation of turbulent channel flows by the variational multiscale method, Phys. Fluids 13 (2001) 1784–1799.
- [18] T. Iliescu, W.J. Layton, Approximating the larger eddies in fluid motion III: the Boussinesq model for turbulent fluctuations. An. Ştiinţ. “Al. I. Cuza” Iaşi Tomul XLIV, Secţ. I a Mat. 44 (1998) 245–261.
- [19] V. John, A numerical study of a posteriori error estimators for convection–diffusion equations, Comput. Methods Appl. Mech. Engrg. 190 (2000) 757–781.
- [20] V. John, Residual a posteriori error estimates for two-level finite element methods for the Navier–Stokes equations, Appl. Numer. Math. 37 (2001) 503–518.
- [21] V. John, Large Eddy Simulation of Turbulent Incompressible Flows, Analytical and Numerical Results for a Class of LES Models, in: Lecture Notes in Comput. Sci. Engrg., vol. 34, Springer, Berlin, 2003.
- [22] V. John, W.J. Layton, Approximating local averages of fluid velocities: The Stokes problem, Computing 66 (2001) 269–287.

- [23] V. John, G. Matthies, MoonNMD—A program package based on mapped finite element methods, *Comput. Visual. Sci.*, submitted for publication.
- [24] S. Kaya, W.J. Layton, Subgrid-scale eddy viscosity models are variational multiscale methods, Technical Report, University of Pittsburgh, 2002.
- [25] O.A. Ladyzhenskaya, New equations for the description of motion of viscous incompressible fluids and solvability in the large of boundary value problems for them, *Proc. Steklov Inst. Math.* 102 (1967) 95–118.
- [26] W.J. Layton, A connection between subgrid scale eddy viscosity and mixed methods, *Appl. Math. Comput.* 133 (2002) 147–157.
- [27] Y. Maday, E. Tadmor, Analysis of the spectral vanishing viscosity method for periodic conservation laws, *SIAM J. Numer. Anal.* 26 (1989) 854–870.
- [28] G. Matthies, Mapped finite elements on hexahedra. Necessary and sufficient conditions for optimal interpolation errors, *Numer. Algorithms* 27 (2001) 317–327.
- [29] J.S. Mullen, P.F. Fischer, Filtering techniques for complex geometry fluid flows, *Comm. Numer. Methods Engrg.* 15 (1999) 9–18.
- [30] W. Rudin, *Functional Analysis*, second ed., in: *International Series in Pure and Applied Mathematics*, McGraw-Hill, New York, 1991.
- [31] P. Sagaut, *Large Eddy Simulation for Incompressible Flows*, Springer, Berlin, 2001.
- [32] J.S. Smagorinsky, General circulation experiments with the primitive equations, *Mon. Weather Review* 91 (1963) 99–164.